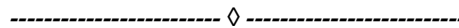


# Effect of boron content on the estimated fracture toughness of FeCo-based bulk metallic glass alloys

S. Zameer Abbas, F. Ahmad Khalid, H. Zaigham

**Abstract:** FeCo-based bulk metallic glass alloy materials with the compositions  $(\text{Fe}_{0.5}\text{Co}_{0.5})_{69-x}\text{Nb}_6\text{B}_{25+x}$  ( $x = 0, 2, 4$ ) were produced by using electric arc melting furnace and suction casting technique. The samples were studied and analyzed in as-cast, and sub- $T_g$  annealed conditions. Fracture toughness of the bulk metallic glass alloys was estimated using the size of the plastically deformed zone that was produced through the bonded interface technique. The estimated values of fracture toughness obtained were comparable to tough bulk metallic glass materials. A maximum value of  $93 \text{ MPa}\sqrt{\text{m}}$  was obtained for the alloy with lowest boron content indicating a composition range with high fracture toughness.

**Key words:** Bulk metallic glass, amorphous material, indentation hardness, shear bands, deformation and fracture, fracture toughness, bonded interface technique



## 1 Introduction

Bulk metallic glasses (BMGs) are a group of materials possessing unique set of properties and have potential to be used in important applications but their Achilles heel is their poor fracture toughness [1-3]. Some Pd and Zr based BMGs possess high fracture toughness whereas other BMG materials are brittle, some of them with fracture toughness values that tend to approach toughness of highly brittle materials like soda-lime glass as reported in [4, 5]. However, testing of fracture toughness using ASTM standard (E399) requires bulk samples of a suitable size and shape for single edge notch beam (SENB) or compact tension (CT) [4]. Nevertheless indentation is one method that allows calculation of fracture toughness of brittle smaller samples through indent corner crack measurement [6-10]. For tougher materials, where microcracks do not form at the indent corners and the size of the sample is small for standard fracture toughness testing, it can be estimated through calculations incorporating plastic zone size (R). This plastic zone is produced underneath a hardness indenter like Vickers [11].

FeCo based BMG alloys with composition  $(\text{Fe}_{0.5}\text{Co}_{0.5})_{69-x}\text{Nb}_6\text{B}_{25+x}$  ( $x = 0, 2, 4$ ) possess high strength and good magnetic properties. A comparison of estimated fracture toughness of three BMG alloys, in both as cast and sub- $T_g$  annealed conditions, is presented to correlate and optimize the composition for better properties. The plastic zones produced in the vicinity and underneath the hardness indent of the samples have been carefully evaluated for the measurement

and comparison of fracture toughness in these BMG alloys.

## 2 Materials and Methods

Alloy buttons (nominal compositions  $(\text{Fe}_{0.5}\text{Co}_{0.5})_{69-x}\text{Nb}_6\text{B}_{25+x}$  ( $x = 0, 2, 4$ )) were prepared by arc melting of high purity elements in a controlled atmosphere arc furnace. Highly pure argon was used for melting and casting of the BMG alloys. Button shaped alloy pieces were produced that were re-melted 4 - 5 times to ensure homogenization. The Bulk metallic glass alloy materials were cast by copper mold suction casting technique in the form of strips that were 1mm thick, 5mm wide and ~20mm long. The samples were tested in as-cast and sub- $T_g$  annealed conditions. These bulk metallic glass (BMG) alloys with  $x = 0, 2, 4$  will be referred to as A1, A2, A3 respectively. Sub- $T_g$  annealing was performed in high vacuum for 30 minutes at 723 K which is well below the glass transition temperatures of these BMG alloys. X-ray diffraction scans were obtained from Philips PW3710 X-ray diffractometer with a step size of  $0.01^\circ$  for 1 second. To observe the shape and size of the plastic zone underneath the hardness indenter, bonded interface technique was employed. Two adjacent surfaces of a sample of a BMG alloy were ground and polished to obtain smoothness and straight edges. Two of these polished samples of the same BMG alloy were bonded together by joining the flat polished sides through a strong polymeric adhesive. This polymeric bonding agent was subsequently dissolved in acetone to separate the polished surfaces after hardness indents were made at the interface with 9.8 N (1.0 kg) load applied for 20 seconds. The thickness of adhesive layer was maintained at  $6 \mu\text{m} \pm 2 \mu\text{m}$ . Images of the BMG samples were taken by using Philips XL 30 scanning electron microscope (SEM).

## 3 Results and Discussion

### 3.1 X-ray Diffraction

- S. Zameer Abbas, Faculty of Materials and Chemical Engineering, GIK Institute, Topi, Pakistan. E-mail: zameer@giki.edu.pk
- F. Ahmad Khalid, UET, Lahore, Pakistan.
- H. Zaigham, FMCE, GIK Institute, Topi, Pakistan.

X-ray diffraction patterns of these alloys in the as cast and annealed conditions were obtained that are shown in figure 1. Absence of peaks in the patterns indicates amorphous nature of the structure in these alloys.

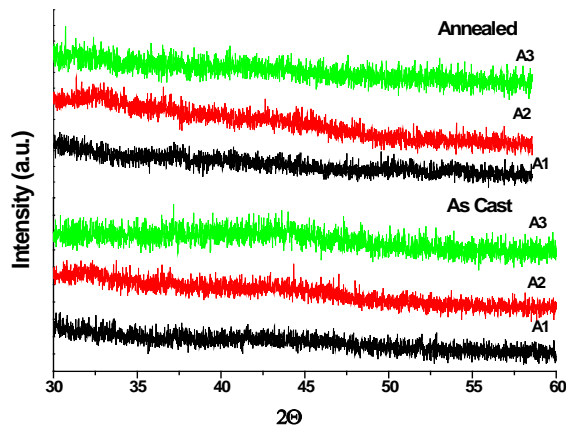


Fig.1 X-ray diffraction patterns of the BMG alloys in the as cast and annealed conditions.

### 3.2 SEM Analysis

Figure 2 (a) shows an indent produced in the BMG alloy at a load of 9.8 N while figure 2 (b) shows an indent produced at the interface with the same load in the bonded interface technique. No microcracks were observed in and around the hardness indents for all the hardness loads employed with a maximum value of 9.8N whereas shear bands can be seen around the indent in figure 2 (a).

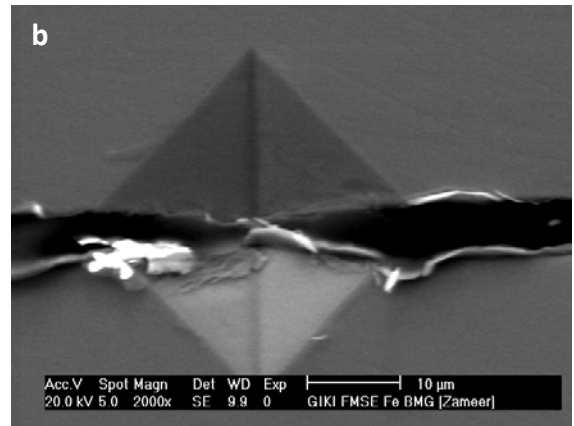
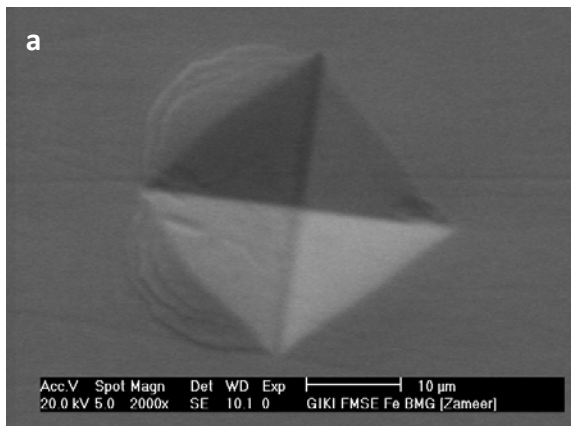


Fig. 2 (a) Hardness indent on the BMG alloy also showing shear bands around edges (b) Hardness indent at the interface of the bonded polished edges of the of the two BMG samples of the same alloy as used in the bonded interface technique.

Figure 3 shows the deformed zones beneath the indents as obtained through the bonded interface technique. The length of the line shown in figure 3 (a) is a measure of the size (R), in micrometers, of the deformed zone. Similarly, size of all the plastic zones of all the alloys were measured through SEM. Semicircular shear bands are visible in both the samples as shown in figure 3. These shear bands result from the localized deformation of the BMG under the applied load [12, 13]. No microcracks were observed within or originating from the deformation zone, an indication of better toughness of the BMG. Microcracking and fragmentation happens in case of brittle BMG materials [11, 14].

### 3.3 Fracture Toughness

In the absence of corner cracks and a suitable sized specimen for standardized testing, the fracture toughness of bulk metallic glass can be roughly estimated through the use of eqn.1 [11, 15].

$$R = \left[ \frac{1}{6\pi} \right] \left[ \frac{K_C}{\sigma_y} \right]^2 \text{ ----- (1)}$$

Where R is the plastic zone size,  $\sigma_y$  is the yield strength,  $K_C$  is fracture toughness.

Table 1 shows fracture toughness values based on the plastic zone size R, calculated using equation 1. Compressive yield strength  $\sigma_y$  has been obtained from the hardness data using a constraint factor of 2.5 [4, 5, 16].

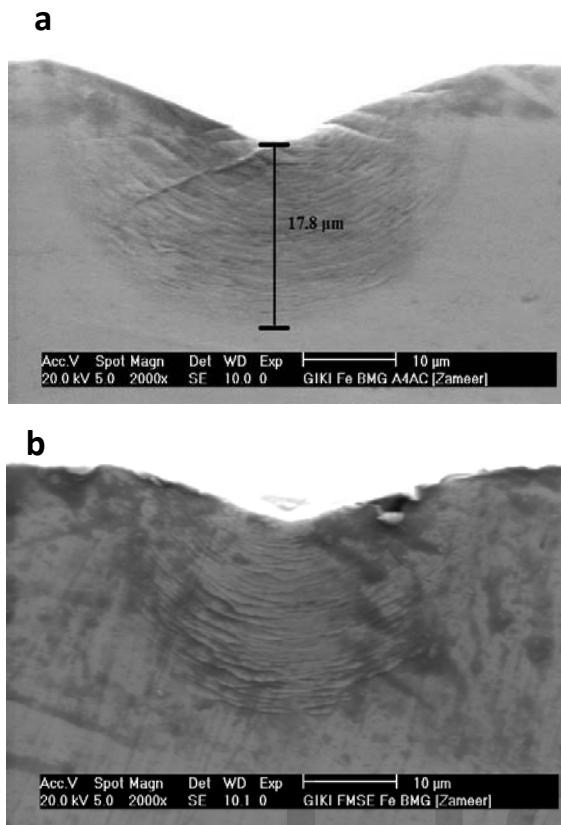


Fig. 3 plastically deformed zones in the alloys that are formed beneath the hardness indent at the interface. Semicircular shear bands are visible both (a) in as cast condition (zone marked) and (b) in sub- $T_g$  annealed condition.

The fracture toughness values obtained from eq.1 are only estimates, which, reveal that these alloys are considerably tough, with values much better than Fe based BMG alloys reported in previous work [5-8, 17]. Even a 30% overestimation will produce a value near  $50 \text{ MPa}\sqrt{\text{m}}$  that is higher than brittle BMGs having values less than  $20 \text{ MPa}\sqrt{\text{m}}$ .

TABLE 1

Hardness, yield strength, and fracture toughness of the as cast and annealed BMGs.

| Alloy | Condition | $\sigma_y$ (MPa) | R ( $\mu\text{m}$ ) | SD   | $K_C$ ( $\text{MPa}\sqrt{\text{m}}$ ) |
|-------|-----------|------------------|---------------------|------|---------------------------------------|
| 1     | As Cast   | 4614             | 20.8                | 0.21 | 91                                    |
|       | Annealed  | 4763             | 20.1                | 0.62 | 93                                    |
| 2     | As Cast   | 4373             | 20.0                | 0.28 | 85                                    |
|       | Annealed  | 4618             | 18.8                | 0.70 | 87                                    |
| 3     | As Cast   | 4567             | 17.0                | 0.36 | 82                                    |
|       | Annealed  | 4692             | 17.4                | 0.42 | 85                                    |

$H_V$  = Vickers hardness,  $\sigma_y$  = Compressive yield strength, R = Deformed zone size, SD = Standard deviation,  $K_C$  = Fracture toughness.

### 3.4 Effect of Boron Content

Fracture toughness has revealed a decreasing trend with a replacement of Fe and Co with boron. The Poisson's ratio of boron is low ( $\nu = 0.21$ ) and an increase in the boron content of the BMG alloy decreases its Poisson's ratio which in turn decreases the toughness [4, 17, 18].

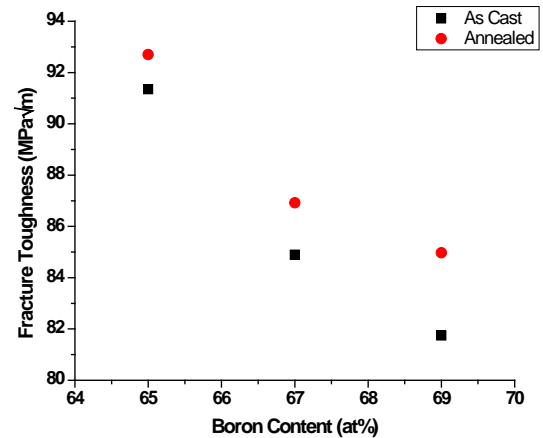


Fig. 4 Fracture toughness as a function of boron content of the BMG alloys in the as cast and annealed conditions.

Sub- $T_g$  annealing is expected to decrease the free volume of the BMG alloys and, therefore, results in an increase in fracture toughness as shown in figure 4. The decrease in toughness, according to equation 1, is due to a decrease in the size of plastically deformed zone (R) formed underneath the hardness indent, that is also given in the table 1.

Increase in the boron content increases the tendency to compound formation thus reducing the toughness of the BMG alloys. There is a large negative difference in the mixing enthalpy values of B with Fe, Co and Nb (Fe-B=  $-26.5 \text{ kJ/mol}$ , Co-B=  $-24.2 \text{ kJ/mol}$ , Nb-B=  $-53.9 \text{ kJ/mol}$ ) that is an indication of its compound forming tendency [19].

## 4 Conclusions

The following conclusions were drawn from this investigation;

1. No microcracks found that were initiated from corners of hardness indents in both as cast and annealed bulk metallic glass alloy samples. Similarly no microcracks were observed within the deformed zone.
2. High fracture toughness values in excess of  $80 \text{ MPa}\sqrt{\text{m}}$  were estimated using size of the deformed zone for both as cast and annealed alloys. The maximum fracture toughness value of  $93 \text{ MPa}\sqrt{\text{m}}$  was obtained for annealed alloy A1.
3. The fracture toughness has revealed an increasing trend with sub- $T_g$  annealing.
4. Fracture toughness values have shown a decreasing trend with an increase in the boron content of the

bulk metallic glass alloy both in as cast and annealed conditions.

## Acknowledgement

This work has been carried out through the funds provided by the higher education commission, Pakistan and Ghulam Ishaq Khan Institute of Engineering Sciences and Technology, Topi, Pakistan.

## References

1. Inoue A, Kong F L, Man Q K, Shen B L, Li R W, Al-Marzouki F. Development and applications of Fe- and Co-based bulk glassy alloys and their prospects. *J Alloy & Compd.* 2014; 615: S2-S8.
2. Inoue A, Takeuchi A. Recent development and application products of bulk glassy alloys. *Acta Mater.* 2011; 59(6): 2243 - 2267.
3. Axinte E. Metallic glasses from alchemy to pure science: Present and future of design, processing and applications of glassy metals. *Mater Design.* 2012; 35(0):518 - 556.
4. Sun B A, Wang W H. The fracture of bulk metallic glasses. *Prog Mater Sc.* 2015; 74: 211 - 307.
5. Wang W H. The elastic properties, elastic models and elastic perspectives of metallic glasses. *Prog Mater Sc.* 2012; 57(3): 487- 656.
6. Madge S V. Toughness of Bulk Metallic Glasses. *Metals.* 2015; 5: 1279 - 1305.
7. Xu T, Li R, Xiao R, Liu G, Wang J, Zhang T. Tuning glass formation and brittle behaviors by similar solvent element substitution in (Mn,Fe)-based bulk metallic glasses. *Mat Sc & Engg A.* 2015; 626: 16 - 26.
8. Keryvin V, Hoang V H, Shen J. Hardness, toughness, brittleness and cracking systems in an iron-based bulk metallic glass by indentation. *Intermetallics.* 2009; 17: 211- 217.
9. Zhang T, Feng Y, Yang R, Jiang P. A method to determine fracture toughness using cube-corner indentation. *Scripta Mater.* 2010; 62: 199 - 201.
10. Ponton C B, Rawlings R D, Vickers indentation fracture toughness test Part 1: Review of literature and formulation of standardized indentation toughness equations. *Mater Sci Tech.* 1989; 5: 865 - 872.
11. Paykani M A, Ahmadabadi M N, Seiffodini A, On the subsurface deformation of two different Fe-based bulk metallic glasses indented by Vickers micro hardness. *Intermetallics.* 2014; 46: 118 - 125.
12. Zhang, H, Jing X, Subhash G, Kecskes L J, Dowding R J. Investigation of shear band evolution in amorphous alloys beneath a Vickers indentation. *Acta Mater.* 2005; 53: 3849 - 3859.
13. Ramamurty U, Jana S, Kawamura Y, Chattopadhyay K. Hardness and plastic deformation in a bulk metallic glass. *Acta Mater.* 2005; 53: 705 - 717.
14. Abbas S Z, Khalid F A, Zaigham H. Indentation and deformation behavior of FeCo-based bulk metallic glass alloys. *Mat Sc & Engg A.* 2016; 654: 426 - 435.
15. Gu X J, Poon S J, Shiflet J G, Lewandowski J J. Compressive plasticity and toughness of a Ti-based bulk metallic glass. *Acta Mater.* 2010; 58(5): 1708-1720.
16. Zhang P, Li S X, Zhang Z F, General relationship between strength and hardness. *Mat Sc & Engg A.* 2011; 529: 62 - 73.
17. Madge S V, Louzguine-Luzgin D V, Lewandowski J J, Greer A L, Toughness, extrinsic effects and Poisson's ratio of bulk metallic glasses. *Acta Mater.* 2012; 60: 4800 - 4809.
18. Lewandowski J J, Shazly M M, Nouri A S. Intrinsic and extrinsic toughening of metallic glasses. *Scripta Mater.* 2006; 54:337 - 341.
19. Takeuchi A, Inoue A. Classification of Bulk Metallic Glasses by Atomic Size Difference, Heat of Mixing and Period of Constituent Elements and Its Application to Characterization of the Main Alloying Element. *Mater T JIM.* 2005;12(46): 2817 - 2829.